Simulating reinforced concrete members. Part 1: partial interaction properties

Oehlers, D. J., Visintin, P., Chen, J-F., & Ibell, T. J. (2014). Simulating reinforced concrete members. Part 1: partial interaction properties. *Proceedings of the ICE - Structures and Buildings*, *167*(11), 646-653. https://doi.org/10.1680/stbu.13.00071

Published in:
Proceedings of the ICE - Structures and Buildings

Document Version:
Publisher's PDF, also known as Version of record

Structures and Buildings
Volume 167 Issue SB11

Simulating reinforced concrete members. Part 1: partial interaction properties
Oehlers, Visintin, Chen and Ibell

ice | proceedings

Proceedings of the Institution of Civil Engineers
Structures and Buildings 167 November 2014 Issue SB11
Pages 646–653 http://dx.doi.org/10.1680/stbu.13.00071
Paper 1300071
Received 16/09/2013 Accepted 26/03/2014
Published online 19/06/2014
Keywords: concrete structures/buildings, structure & design/strength & testing of materials

ice Institution of Civil Engineers publishing

Simulating reinforced concrete members. Part 1: partial interaction properties

Deric J. Oehlers
Emeritus Professor, School of Civil, Environmental and Mining Engineering, University of Adelaide, Adelaide, Australia
Phillip Visintin
Lecturer, School of Civil, Environmental and Mining Engineering, University of Adelaide, Adelaide, Australia
Jian-Fei Chen
Professor, School of Planning, Architecture and Civil Engineering, Queen's University Belfast, Belfast, UK
Tim J. Ibell
Professor, Department of Architecture and Civil Engineering, University of Bath, Bath, UK

Reinforced concrete members are extremely complex under loading because of localised deformations in the concrete (cracks, sliding planes) and between the reinforcement and concrete (slip). An ideal model for simulating behaviour of reinforced concrete members should incorporate both global behaviour and the localised behaviours that are seen and measured in practice; these localised behaviours directly affect the global behaviour. Most commonly used models do not directly simulate these localised behaviours that can be seen or measured in real members; instead, they overcome these limitations by using empirically or semi-empirically derived strain-based pseudo properties such as the use of effective flexural rigidities for deflection; plastic hinge lengths for strength and ductility; and energy-based approaches for both concrete softening in compression and concrete softening after tensile cracking to allow for tension stiffening. Most reinforced concrete member experimental testing is associated with deriving these pseudo properties for use in design and analysis, and this component of development is thus costly. The aim of the present research is to reduce this cost substantially. In this paper, localised material behaviours and the mechanisms they induce are described. Their incorporation into reinforced concrete member behaviour without the need for empirically derived pseudo properties is described in a companion paper.

Notation

A_c	cross-sectional area of concrete
A_r	cross-sectional area of reinforcement
d	depth of section
$d\delta/dx$	slip strain
E_c	concrete modulus
E_r	reinforcement modulus
EI	flexural rigidity
f_c	concrete compressive strength
f_t	concrete tensile strength
L	length of cylinder or prism
M	moment
N_c	component of P_c normal to sliding plane
P	axial force in reinforcement at a crack; applied load
P_c	axial force in concrete element
S_{cr}	primary crack spacing
T_c	component of P_c along sliding plane
w	crack width; widening across sliding plane
α	wedge angle
Δ	reinforcement slip relative to crack face; half crack width
Δd	lateral slip
ΔL	longitudinal slip
ΔP	change in P due to shear sliding
$\Delta\sigma_n$	change in σ_n due to shear sliding
δ	slip along sliding plane
δ_1	slip corresponding to τ_{max}
δ_{max}	slip when τ tends to zero
ε	strain
ε_a	axial strain
ε_{asc}	strain in ascending branch
ε_{des}	strain in descending branch
ε_{eff}	effective strain
ε_{mat}	material strain
ε_r	axial strain in reinforcement
ν_c	Poisson ratio of concrete material
σ	stress
σ_a	axial stress
σ_n	stress normal to sliding plane
σ_s	stress at start of softening
τ	shear stress
τ_{max}	maximum shear strength of bond
χ	curvature

1. Introduction

Reinforced concrete (RC) has been a great invention in making good use of both concrete and steel, but the low tensile strength of concrete means that most RC members work with localised deformations due to cracks and sliding planes, and with slip between the reinforcement and concrete, characteristics which are

seen and measured in practice. The localised nature of these deformations makes the behaviour of RC members extremely complex as it is these localised behaviours that control the global behaviour of RC members. Thus it is very important that these behaviours are simulated (Oehlers, 2010a; Oehlers *et al.*, 2011a, 2011b, 2012) in order to accurately replicate the global behaviours.

For RC members, the localised behaviours are: the slip between the reinforcement and the adjacent concrete, which controls crack spacings and widths and the variation in tensile strain along the cracked region (Chen *et al.*, 2007, 2012; Gupta and Maestrini, 1990; Knight *et al.*, 2013; Muhamad *et al.*, 2011, 2013; Teng *et al.*, 2006; Visintin *et al.*, 2012; Wu *et al.*, 1991); the formation of wedges in concrete compression zones (Harmon *et al.*, 1998; Mohamed Ali *et al.*, 2010; Van Mier and Man, 2009), which allows large compressive deformations to be accommodated by sliding along the concrete to concrete wedge interface (Chen *et al.*, 2012; Mohamed Ali *et al.*, 2010); the rigid body shear sliding across a concrete to concrete interface associated with shear failure of a member (Haskett *et al.*, 2011; Lucas *et al.*, 2011); discrete zones of high rotation often associated with wedge sliding and large crack widths and referred to as plastic hinges (Baker, 1956; Corley, 1966; Haskett *et al.*, 2009a, 2009b; Mattock, 1967; Panagiotakos and Fardis, 2001) and which affect moment redistribution (Oehlers *et al.*, 2010b; Haskett *et al.*, 2010); and time-dependent deformations such as those due to creep, shrinkage, relaxation and deterioration (Bazant, 1972; Bresler and Selna, 1964; Faber, 1927; Visintin *et al.*, 2013).

The behaviour of RC members is governed by the strain-based material properties, such as the commonly used stress–strain (σ–ε) relationship. However, the behaviour is also governed by slip across interfaces and these will be referred to as the partial-interaction (PI) material properties, which include the bond-slip (τ/δ) between the reinforcement and its adjacent concrete (Seracino *et al.*, 2007; Wu and Zhao, 2012) and less understood shear-friction properties across a concrete–concrete sliding plane (Birkeland and Birkeland, 1966; Haskett *et al.*, 2011; Hofbeck *et al.*, 1969; Mansur *et al.*, 2008). It is these PI material properties which make the local behaviour and consequently the global behaviour of RC very complex and difficult to simulate, particularly using strain-based approaches, such as continuum-based approaches without due consideration of deformation localisation.

To help simplify the incredible complexity of RC member behaviour, in this paper an attempt is made to

- define pseudo properties as opposed to real properties
- explain the range of material properties and in particular the PI material properties which are associated with slip
- explain the mechanisms by which these PI material properties cause tension stiffening, concrete softening and shear sliding

and then a companion paper (Oehlers *et al.*, 2014) shows how these PI material properties and mechanisms can be included in RC member analyses.

2. Definition of pseudo properties

A material property is defined here as the behaviour of a relatively small element of the material that can be applied at discrete points in a model such as the σ–ε relationship. With this in mind, the pseudo material property is defined here as a property, given in material terms (such as in terms of stress and strain) that not only allow for material behaviour but also for the mechanics within an element or small region of the member, as would occur, for example, with tension stiffening. Hence, the pseudo material property can vary not only with variations in the material properties but also with variations in the mechanics within an element. Pseudo material properties can be derived through mechanics but are often quantified through experimental testing.

A sectional property is the behaviour of a section of a member that can be derived through mechanics, for example the flexural rigidity (EI) which depends on both the material modulus and geometries of the section. A pseudo sectional property is defined here as a sectional property that allows for the mechanics of a segment or small length of the member, as opposed to just that at a section; an example is the effective flexural rigidity commonly used in deflection calculations. Hence, pseudo sectional properties can vary with material properties, geometries of the section, the mechanisms within the member in the vicinity of the section and under different loadings. Pseudo sectional properties may be derived through mechanics but are usually determined either directly through experimental testing or a component of the mechanics model is determined through experimental testing such as hinge lengths.

3. Material properties for RC mechanisms

Two types of material properties are required for simulating the failure mechanisms of RC structures: (*a*) the commonly used strain-based material properties, such as the direct relationship between the axial stress and axial strain (σ_a/ε_a) and its associated time-dependent properties of shrinkage, creep, relaxation and deterioration, which may be referred to as continuum-based properties; and (*b*) the less used and often less understood PI material properties associated with slip across an interface such as the bond-slip and shear-friction properties which could also be referred to as discrete deformation properties.

3.1 Strain-based material properties

A strain-based material property is simply the relationship between the stress and strain of an element of the material, which can then be applied at discrete points in the analysis of a member. However, determining the strain-based material properties may not be as simple as it first appears. As an example, consider a standard compression test on a cylinder of concrete, as in Figure 1. Attaching relatively small strain gauges around the circumference in line with the length L of the cylinder will provide a local or material ascending stress–strain relationship such as O-A-B in Figure 2, which peaks at the maximum strength f_c.

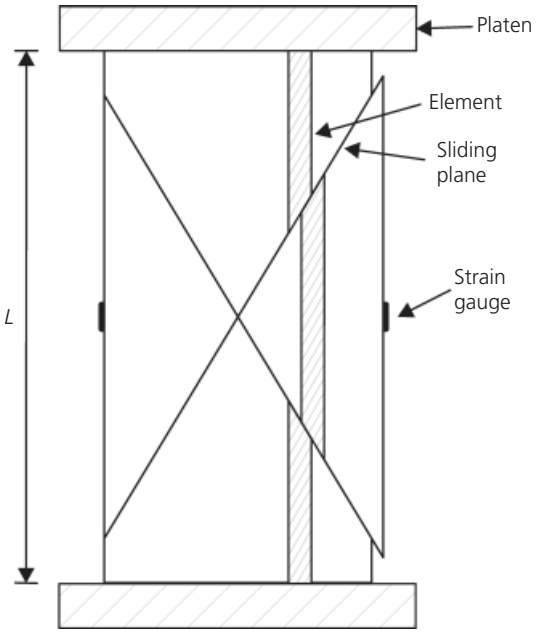

Figure 1. Concrete compression test

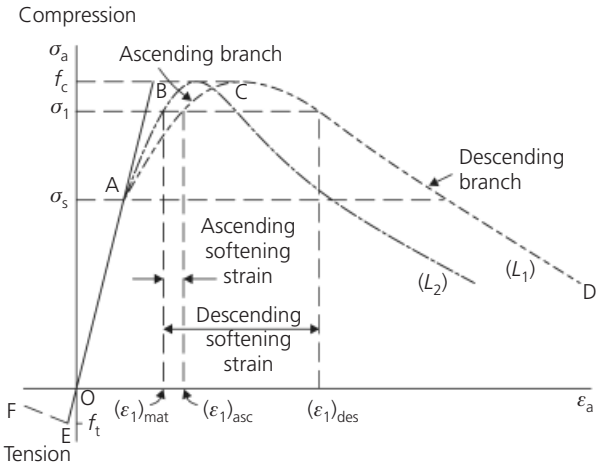

Figure 2. Concrete deformation in strains

In contrast to using the local strains as measured through strain gauges in Figure 1, measuring the overall contraction between platens at the ends of the cylinder and dividing these contractions by the length of the cylinder L will give a global or pseudo material stress–strain relationship such as O-A-C-D for the specimen of length L_1 in Figure 2. The global stress–strain relationship is characterised by a falling branch even though this has not occurred in the material stress–strain relationship O-A-B. At point A on the ascending branch, the globally measured strains diverge from the locally measured strains, that is strain softening occurs such as $(\varepsilon_1)_{asc} - (\varepsilon_1)_{mat}$ at stress level σ_1 in the ascending branch, which increases substantially to $(\varepsilon_1)_{des} - (\varepsilon_1)_{mat}$ in the falling branch.

No matter whether the strain-based properties are real material properties or pseudo material properties, the descending branch in Figure 2 poses a problem in simulations because it is necessary to define a boundary between those elements on the ascending branch and those on the descending branch. For example, an element at stress level σ_1 in Figure 2 may be softening with a strain $(\varepsilon_1)_{des}$. However, an adjacent element with the same stress σ_1, that is required for equilibrium, may still be on the ascending branch with a strain $(\varepsilon_1)_{asc}$. Hence there is a step change in the strain $(\varepsilon_1)_{des} - (\varepsilon_1)_{asc}$ and the boundary where this occurs needs to be defined as in the use of plastic hinge lengths in moment–curvature (M–χ) analyses or elements of a discrete size for finite-element analyses.

3.2 PI material properties

The partial interaction material properties are associated with slip across an interface. When the interface is between two adjacent concrete elements, then these are the shear-friction properties. When the interface is between reinforcement and the adjacent concrete then these are the bond-slip properties.

3.2.1 Shear-friction properties

The shear-friction mechanism is the rigid body movement of adjacent concrete elements across a potential sliding plane, as illustrated in Figure 3, where τ is the shear stress along the sliding plane, δ is the relative slip between the adjacent concrete elements, σ_n is the stress normal to the sliding plane, that is the active confinement applied across the sliding plane, and w is the relative separation of the adjacent elements due to shear sliding.

The sliding plane in Figure 3 can lie through an already formed crack, in which case the element faces are simply the crack faces and w is the width of the crack that is the distance between element faces. The roughness or irregularity of the crack faces will cause the slip δ induced by the shear stress τ to widen the

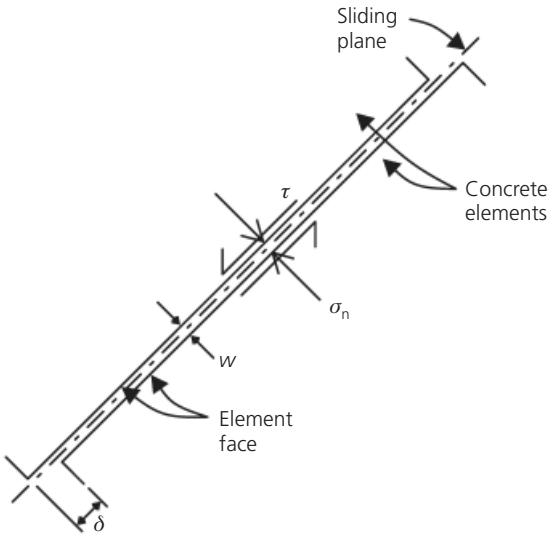

Figure 3. Shear friction mechanism

crack width w; this mechanism is referred to as aggregate interlock. Alternatively, the sliding plane can lie through uncracked concrete. In this case, the shear forces can induce a distinctive herringbone formation of cracks and it is the rotation of the struts between the herringbone formation which induces both δ and w and eventually leads to a crack along the sliding plane.

The shear-friction properties, that is the interaction between the parameters τ, σ_n, δ and w in Figure 3, are often depicted as in Figure 4 (Haskett *et al.*, 2011) and can be applied at discrete points in the analysis of a member. It is the combination of these parameters, such as those joined by a dashed line in Figure 4, that is τ_x, $(\sigma_n)_x$, δ_x and w_x which occur together at a discrete point. The shear-friction properties not only depend on the concrete compressive strength but also on other parameters such as the aggregate size and strength and mortar properties.

3.2.2 Bond-slip properties

Consider reinforcement attached to concrete as depicted in Figure 5(a). Prior to cracking there is full interaction, that is there is no slip between the reinforcement and the adjacent concrete; there could be shear stresses across the interface due to the moment gradient which can be derived from the elementary mechanics of the shear flow (VAy/Ib) approach. However, when the first or initial crack forms as in Figure 5(a), slip must occur between the reinforcement and the adjacent concrete, that is partial interaction, to allow the crack to widen to w. The element to the right of the crack is shown in Figure 5(c). The force in the reinforcement is P and this induces slip along the interface δ (as shown in Figure 5(d)), which has a maximum value of Δ at the crack face and gradually diminishes to zero where there is full interaction. This slip is resisted by interface shear τ, as illustrated in Figure 5(e), which is generally at least an order of magnitude greater than that due to longitudinal shear when there is full interaction. The relationship between the interface slip δ and shear stress τ at a discrete point is the bond-slip property required for partial interaction analyses.

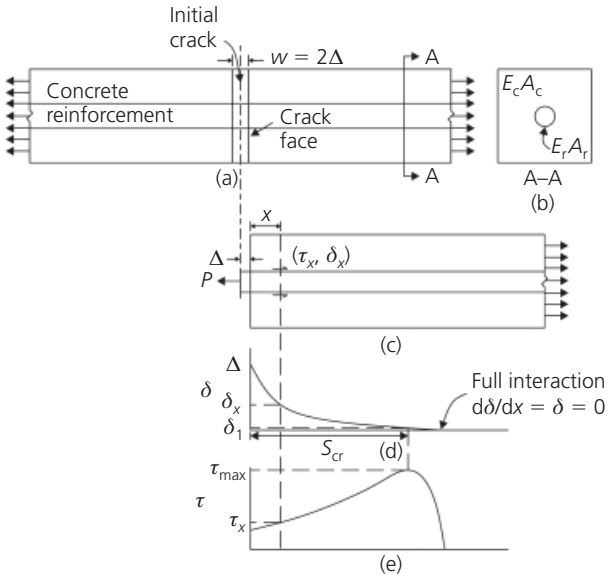

Figure 5. Bond-slip mechanism: (a) prism; (b) section; (c) equilibrium; (d) slip distribution; (e) shear–stress distribution

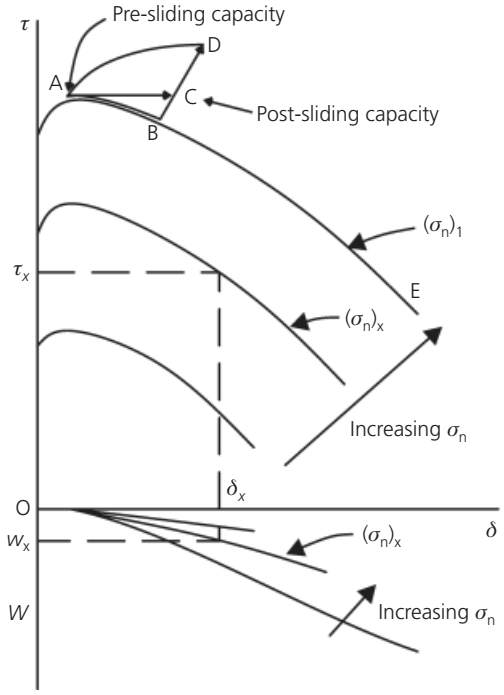

Figure 4. Shear-friction properties

The bond-slip properties applicable at discrete points are invariably derived from pull-out tests. Typical shapes of these variations for externally bonded plates (EB), near-surface-mounted strips (NSM) and ribbed bars with plenty of cover are shown in Figure 6 (Seracino *et al.*, 2007; Wu and Zhao, 2012), where the maximum shear stress τ_{max} occurs at a slip δ_1 and the shear strength tends to zero at a slip δ_{max}, which is also a measure of the bond ductility and beyond which there may be a frictional component not shown. The bond strength τ_{max} and ductility δ_{max}

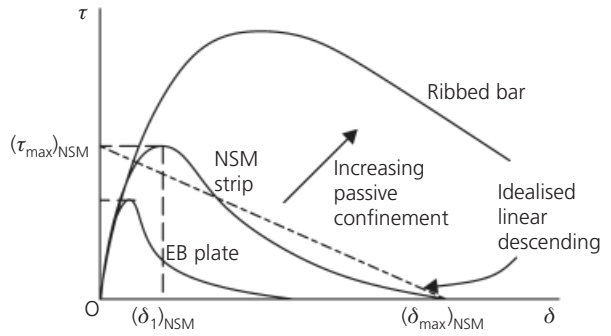

Figure 6. Bond-slip properties

increase with reinforcement embedment; the EB plates being the weakest and least ductile, whereas the ribbed bars are the strongest and most ductile. This is because increasing embedment increases the passive confinement across the interface sliding plane. For example, when the reinforcing bar in Figure 5(c) is pulled out of the concrete, the bar ribs act in the same way as aggregate interlock in Figure 3, causing a separation w between the bar and the adjacent concrete. This separation is resisted by the body of the concrete surrounding the reinforcement as in Figure 5(b), inducing normal or confining stresses σ_n across the concrete–reinforcement interface. These confining stresses only exist if slip occurs and, hence, they are passive. Therefore, the bond-slip τ/δ properties in Figure 6 are similar to the shear-friction τ/δ properties in Figure 4 except that the latter properties are due to active confinement whereas the former are due to passive confinement.

4. Partial interaction mechanisms

The PI material properties described in Section 3 cause the following PI mechanisms within RC members which are accommodated in strain-based analyses through the use of pseudo material properties.

4.1 Tension stiffening mechanism

Consider the RC prism in Figure 5(a) which consists of reinforcement of cross-sectional area A_r and modulus E_r encased by a concrete prism of area A_c and modulus E_c such that the axial rigidity of the prism prior to cracking is $E_rA_r + E_cA_c$. After a crack has formed, as shown in Figure 5(a), the axial rigidity of the prism reduces but is greater than that of the reinforcement alone E_rA_r. This increase in stiffness is referred to as tension stiffening and can be allowed for in strain-based analyses by the use of a pseudo material tension softening such as the path E-F in Figure 2 after the concrete has cracked in tension at f_t.

After the initial crack has developed in the prism in Figure 5(a), the total force in the prism is resisted by the force in the reinforcement P at the crack face, as shown in Figure 5(c). The reinforcement force P induces an interface slip δ which has a maximum value at the crack face of Δ. This interface slip diminishes from Δ at the crack face to zero at the distance S_{cr} from the crack face where both the slip δ and the slip–strain $d\delta/dx$ reduce to zero, which is the full interaction boundary condition. At S_{cr}, the stress in the concrete reaches its maximum value and remains constant beyond. Hence the next crack, which will be referred to as the primary crack, can occur anywhere beyond S_{cr} from the crack face. The distance S_{cr} is, therefore, the minimum crack spacing of primary cracks and if there is a moment gradient in the beam it will be close to the actual crack spacing.

When the primary cracks have formed as shown in Figure 7(a), the mechanism changes from that in Figure 5(c) to that in Figure 7(b), where the prism is now symmetrically loaded and is of length S_{cr}. The variations in slip and shear in Figures 7(c) and 7(d) depend on the bond-slip properties in Figure 6. However,

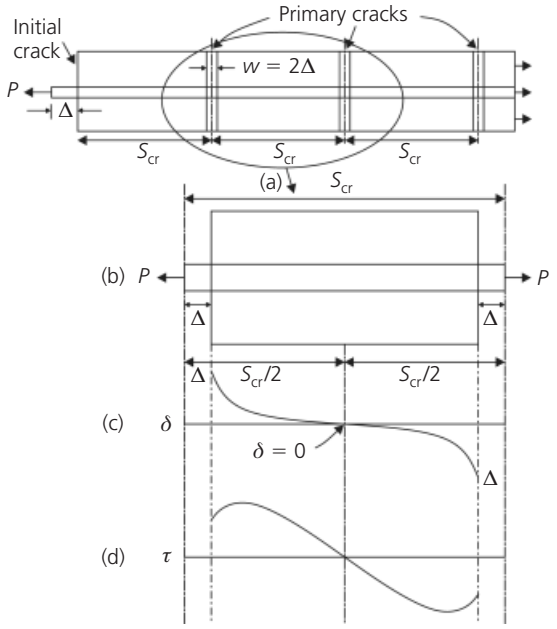

Figure 7. Tension-stiffening mechanism: (a) prism; (b) primary cracks; (c) slip; (d) bond

through the symmetry of loading in Figure 7(b), the interface slip and interface shear are zero at mid-length as shown and where the stress in the concrete is at its maximum. Hence if the bond is sufficiently strong and stiff and the reinforcement force sufficiently large to cause secondary cracking, the secondary cracks will occur midway between the primary flexural cracks, so that in regions where secondary cracking occurs the crack spacing reduces to $S_{cr}/2$.

4.2 Concrete softening mechanism in compression

Consider the prism in Figure 8 of length L, depth d and cross-sectional area into the page of A_c, which is subjected to a uniform axial compressive stress σ_a. On gradual loading, the contraction of the prism is governed by the material strain along the path O-A in Figure 2 where the stress at A, σ_s, is the stress at the commencement of softening. When the axial stress exceeds the stress at the commencement of softening σ_s in Figure 2, a non-material deformation begins to develop, usually along a single plane of weakness at an angle α, as in Figure 8, where the angle of this sliding plane α depends on the Mohr–Coulomb frictional component of concrete and is usually about 26° (Harmon *et al.*, 1998; Mattock, 1974; Mohamed Ali *et al.*, 2010; Rutland and Wang, 1997; Van Mier and Man, 2009). The longitudinal deformation due to straining of the concrete material is given by σ_aL/E_c where E_c is the modulus of the concrete at the stress σ_a from the path O-A-B in Figure 2.

The longitudinal deformation due to sliding, ΔL in Figure 8, can be determined from the shear-friction mechanism in Figure 3 and the shear-friction properties in Figure 4. The axial force in the prism P_c in Figure 8 is $A_c\sigma_a$ and this can be resolved into a shear

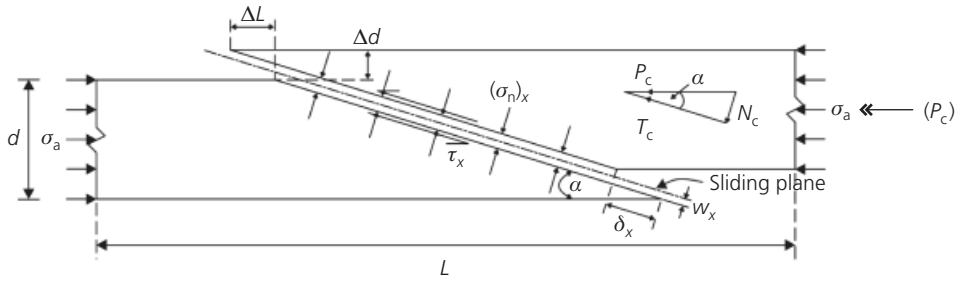

Figure 8. Concrete softening mechanism

force T_c from which the shear stress along the sliding plane τ_x can be derived, and a force normal to the sliding plane N_c from which the normal stress $(\sigma_n)_x$ can be derived. Hence from the shear-friction material properties such as in Figure 4 the slip δ_x and crack width w_x can be derived when σ_a is applied. From the geometry of the sliding plane, the axial contraction ΔL can be derived. This axial contraction due to sliding ΔL in Figure 8 is independent of the length of the prism L.

The total contraction of the prism in Figure 8 is that due to material contraction $\sigma_a L/E_c$, that is $\varepsilon_a L$ where ε_a is the material strain in the concrete, plus that due to shear sliding ΔL. Dividing this total contraction by the length of the prism L gives an effective axial strain ε_{eff} of $\varepsilon_a + \Delta L/L$ where the first component ε_a is the material strain and the second component $\Delta L/L$ is a pseudo-strain which, as can be seen, is size dependent and which is the softening strain in Figure 2. Applying the same logic to the lateral expansion in Figure 8, the effective lateral strain is $\nu_c\varepsilon_a + \Delta d/d$ where the former component is attributable to material expansion and the latter is due to slip.

4.3 Shear sliding mechanism

The behaviour of a sliding plane that intercepts reinforcement, as illustrated in Figure 9(a), is next considered. The shear is transferred across the sliding plane by the shear-friction mechanism in Figure 3, which is enhanced by confinement owing to the reinforcing bar, which is referred to as the shear sliding mechanism, and also by dowel action.

The shear sliding mechanism is illustrated in Figure 9(a) (Lucas *et al.*, 2012). The shear stress τ causes a slip δ which through the shear-friction mechanism in Figure 3 causes the widening w as shown in Figure 9(a). This widening is resisted by the reinforcing bar through the tension-stiffening mechanism illustrated in Figure 5(c), where in this case the boundary condition can vary depending on the length of the reinforcement; this is shown in Figure 9(c) where the first boundary condition $d\delta/dx = \delta = 0$ is the full-interaction boundary condition; the second boundary condition $\delta = 0$ is when the end of the bar is fully anchored; and the third boundary condition $\varepsilon_r = 0$ when the end of the bar is free to slide. This causes a tensile increase in the force in the reinforcement ΔP as shown in Figure 9(b) and an equal and opposite increase in the compressive confinement force across the

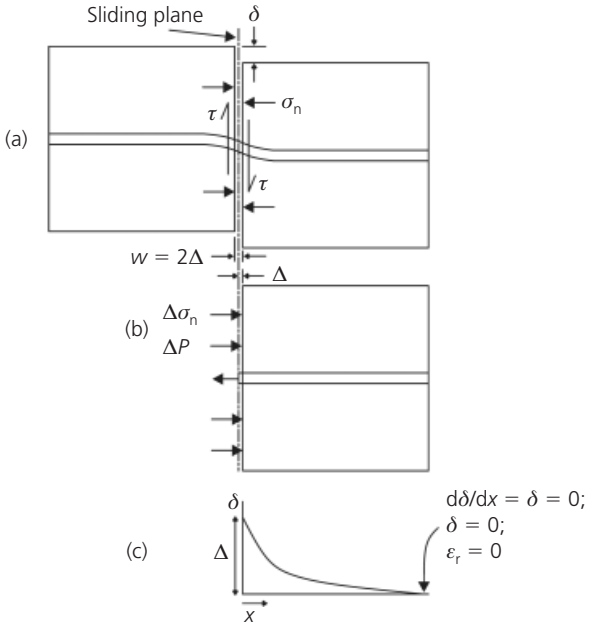

Figure 9. Shear sliding mechanism: (a) shear sliding; (b) equilibrium; (c) slip distribution

sliding plane which can be converted to an increase in the compressive confinement stress, $\Delta\sigma_n$. It can be seen that this is an example of passive confinement, as the confinement gradually builds up with slip.

It is important to realise that the tensile increase in the reinforcement force ΔP in Figure 9(b) is exactly equal to the increase in the compressive confining force $\Delta\sigma_n A_c$ and that both of these resulting forces are in line. Hence there is no change in the overall equilibrium of the member, but what does increase is the confinement across the sliding plane, which can make shear sliding not only stronger but more ductile. Prior to shear sliding, there could already be either a tensile or compressive force in the reinforcement and the tensile increase ΔP is added to this algebraically. Similarly, prior to sliding, there could be either a compressive or tensile force normal to the sliding plane and once again the compressive increase $\Delta\sigma_n$ is added to this algebraically. It can be seen that confinement is now no longer an esoteric phenomenon but a force on a sliding plane that can be quantified

and the benefits of which, such as increased strength or ductility, can also be quantified.

If the normal stress σ_n to the sliding plane in Figure 9(a) remained constant such as at $(\sigma_n)_1$ along A-B-E in Figure 4, then sliding would cause a reduction in the shear stress τ from, say, points A to B as shown, so that the maximum shear capacity is the pre-sliding capacity. However, the reinforcement increases the confinement by $\Delta\sigma_n$ in Figure 9(b) to $(\sigma_n)_1 + \Delta\sigma_n$ in Figure 4 as explained, which will increase the shear capacity such as to point C or point D depending on the increase in confinement. Hence the post-sliding capacity can be larger depending on the shear sliding behaviour. Hence the pre-sliding capacity is always equal to or a lower bound to the shear capacity and the shear sliding mechanism always improves the ductility.

The sliding plane resists shear through the shear sliding mechanism, which increases the tensile component of the reinforcement force ΔP in Figure 9. The shear along the sliding plane is also resisted by dowel action, which correspondingly increases the axial tensile stresses within the reinforcing bars. The reinforcing bar has to resist both components; that is, they are not resisted independently by the reinforcement. Hence if dowel action is assumed to resist part of the shear then only a part of the capacity of the reinforcing bar is available to resist shear sliding and vice versa. How much is resisted by each component is difficult to quantify. A simple approach is to assume that all of the shear is resisted by the shear sliding mechanism and ignore the dowel action, and this appears to give good results.

5. Conclusion

A large amount of testing in the development of RC products and their associated design rules is required to provide pseudo material properties for the use of strain-based analysis techniques. It has been shown in this paper that this is due to partial interaction material properties caused by slip between the reinforcement and concrete and between cracked and uncracked concrete interfaces. The localised mechanisms that these partial interaction material properties induce in RC members has also been identified in mechanics terms. Hence it is now possible to simulate, with the help of partial interaction material properties, the pseudo material properties often determined empirically and required for strain-based approaches. This mechanics-based alternative approach will require extra testing to determine the partial interaction material properties, but once these material properties have been quantified there is no limit to their application, because they are generic properties that can then be used to derive pseudo material properties for any numerical simulation. This alternative approach is in contrast to the current approach of empirically determining pseudo material properties which are generally of limited accuracy, often very conservative and can only be used within the bounds of the testing regimes from which they were derived and, hence, require a large and ongoing amount of testing. The development of mechanics-based pseudo material properties not only obviates the need to determine them through experimental testing but allows the development of mechanics models for use in RC member analysis, which is the subject of the companion paper.

Acknowledgement

The financial support of the Australian Research Council ARC Discovery project DP0985828 ‘A unified reinforced concrete model for flexure and shear’ is gratefully acknowledged.

REFERENCES

Baker ALL (1956) *Ultimate Load Theory Applied to the Design of Reinforced and Prestressed Concrete Frames*. Concrete Publications, London, UK.

Bazant ZP (1972) Prediction of concrete creep effects using age-adjusted effective modulus method. *ACI Journal* **69(4)**: 323–217.

Birkeland PW and Birkeland HW (1966) Connections in precast concrete construction. *ACI Journal Proceedings* **63(3)**: 345–368.

Bresler B and Selna L (1964) Analysis of time dependent behaviour of reinforced concrete structures. In *Proceedings of the Symposium of Creep in Concrete*. American Concrete Institute, Farmington Hills, MI, USA, ACI Special Publication SP9(5), pp. 115–128.

Chen GM, Chen JF and Teng JG (2012) Behaviour of FRP-to-concrete interfaces between two adjacent cracks: a numerical investigation on the effect of bondline damage. *Construction and Building Materials* **28(1)**: 584–591, http://dx.doi.org/10.1016/j.conbuildmat.2011.08.074.

Chen JF, Yuan H and Teng JG (2007) Debonding failure along a softening FRP-to-concrete interface between two adjacent cracks in concrete members. *Engineering Structures* **29(2)**: 259–270.

Chen Y, Visintin P, Oehlers DJ and Johnson AU (2014) Size dependent stress–strain model for unconfined concrete. *ASCE Structures* **140(4)**: http://dx.doi.org/10.1062/(ASCE)ST.1943-S41X.0000869.

Corley GW (1966) Rotation capacity of reinforced concrete beams. *ASCE Journal of the Structural Division* **92(10)**: 121–146.

Faber O (1927) Plastic yield, shrinkage and other problems of concrete and their effects on design. *Minutes of the Proceedings of the Institute of Civil Engineers, Part I* **225**: 27–73.

Gupta AK and Maestrini SR (1990) Tension stiffening model for reinforced concrete bars. *Journal of Structural Engineering* **116(3)**: 769–790.

Harmon TG, Ramakrishnan S and Wang EH (1998) Confined concrete subjected to uniaxial monotonic loading. *Journal of Engineering Mechanics* **124(12)**: 1303–1309.

Haskett M, Oehlers DJ, Mohamed Ali MS and Wu C (2009a) Rigid body moment–rotation mechanism for reinforced concrete beam hinges. *Engineering Structures* **31(5)**: 1032–1041.

Haskett M, Oehlers DJ and Mohamed Ali Wu C (2009b) Yield

penetration hinge rotation in reinforced concrete beams. *ASCE Structural Journal* **135(2)**: 130–138.

Haskett M, Oehlers DJ and Mohamed Ali MS (2010) Design for moment redistribution in RC beams retrofitted with steel plates. *Advances in Structural Engineering* **13(2)**: 379–391.

Haskett M, Oehlers DJ, Mohamed Ali MS and Sharma SK (2011) Evaluating the shear-friction resistance across sliding planes in concrete. *Engineering Structures* **33(4)**: 1357–1364.

Hofbeck JA, Ibrahim IO and Mattock AH (1969) Shear transfer in reinforced concrete. *ACI Journal Proceedings* **66(2)**: 119–128.

Knight D, Visintin P, Oehlers DJ and Jumaat MZ (2013) Incorporating residual strains in the flexural rigidity of RC members with varying degree of prestress and cracking. *Advances in Structural Engineering* **16(10)**: 1701–1718.

Lucas W, Oehlers DJ and Mohamed Ali MS (2011) Formulation of a shear resistance mechanism for inclined cracks in RC beams. *ASCE Journal of Structural Engineering* **137(12)**: 1480–1488.

Lucas W, Oehlers DJ, Mohamed Ali MS and Griffith MC (2012) The FRP reinforced shear-friction mechanism. *Advances in Structural Engineering* **15(4)**: 615–623.

Mansur MA, Vinayagam T and Tan KH (2008) Shear transfer across a crack in reinforced high-strength concrete. *Journal of Materials in Civil Engineering* **20(4)**: 294–302.

Mattock AH (1967) Discussion of rotational capacity of reinforced concrete beams by W. D. G. Corley. *Journal of the Structural Division, ASCE* **93(2)**: 519–522.

Mattock AH (1974) Shear transfer in concrete having reinforcement at an angle to the shear plane. In *Shear in Reinforced Concrete*. American Concrete Institute, Farmington Hills, MI, USA, ACI Special Publication SP42, pp. 17–42.

Mohamed Ali MS, Oehlers DJ and Griffith MC (2010) The residual strength of confined concrete. *Advances in Structural Engineering* **13(4)**: 603–618.

Muhamad R, Mohamed Ali MS, Oehlers DJ and Sheikh AH (2011) Load–slip relationship of tension reinforcement in reinforced concrete members. *Engineering Structures* **33(4)**: 1098–1106.

Muhamad R, Oehlers DJ and Mohamed Ali MS (2013) Discrete rotation deflection of reinforced concrete beams at serviceability. *Proceedings of the Institution of Civil Engineers – Structures and Buildings* **166(3)**: 111–124.

Oehlers DJ (2010a) The hunt for the elusive concept. *Advances in Structural Engineering* **13(5)**: 755–772, Len Hollaway's special edition.

Oehlers DJ, Haskett M, Mohamed Ali MS and Griffith MC (2010b) Moment redistribution in reinforced concrete beams. *Proceedings of the Institution of Civil Engineers – Structures and Buildings* **163(3)**: 165–176.

Oehlers DJ, Haskett M, Mohamed Ali MS, Lucas W and Muhamad R (2011a) Our obsession with curvature in reinforced concrete modelling. *Advances in Structural Engineering* **14(3)**: 399–412.

Oehlers DJ, Mohamed Ali MS, Haskett M *et al.* (2011b) FRP reinforced concrete beams – a unified approach based on IC theory. *Composites for Construction, ASCE* **15(3)**: 293–303.

Oehlers DJ, Mohamed Ali MS, Griffith MC, Haskett M and Lucas W (2012) A generic unified reinforced concrete model. *Proceedings of the Institution of Civil Engineers – Structures and Buildings* **165(1)**: 27–49.

Oehlers DJ, Visintin P, Chen JF and Ibell TJ (2014) Simulating reinforced concrete members. Part 2: displacement based analyses. *Proceedings of the Institution of Civil Engineers – Structures and Buildings* http://dx.doi.org/10.1680/stbu.13.00072.

Panagiotakos TB and Fardis MN (2001) Deformations of reinforced concrete members at yielding and ultimate. *ACI Structural Journal* **98(2)**: 135–148.

Rutland CA and Wang ML (1997) The effects of confinement on the failure orientation in cementitious materials experimental observations. *Cement and Concrete Composites* **19(2)**: 149–160.

Seracino R, Raizal Saifulnaz MR and Oehlers DJ (2007) Generic debonding resistance of EB and NSM plate-to-concrete joints. *Composites for Construction, ASCE* **11(1)**: 62–70.

Teng JG, Yuan H and Chen JF (2006) FRP-to-concrete interfaces between two adjacent cracks: theoretical model for debonding failure. *International Journal of Solids and Structures* **43(18–19)**: 5750–5778, http://dx.doi.org/10.1016/j.ijsolstr.2005.07.023.

Van Mier JGM and Man HK (2009) Some notes on microcracking, softening, localization, and size effects. *International Journal of Damage Mechanics* **18(3)**: 283–309.

Visintin P, Oehlers DJ, Wu C and Griffith MC (2012) The reinforcement contribution to the cyclic behaviour of reinforced concrete beam hinges. *Earthquake Engineering and Structural Dynamics* **41(12)**: 1591–1608.

Visintin P, Oehlers DJ and Haskett M (2013) Partial-interaction time dependent behaviour of reinforced concrete beams. *Engineering Structures* **49(April)**: 408–420.

Wu Z, Yoshikawa H and Tanabe T (1991) Tension stiffness model for cracked reinforced concrete. *Journal of Structural Engineering* **117(3)**: 715–732.

Wu YF and Zhao XM (2012) Unified bond stress–slip model for reinforced concrete. *Journal of Structural Engineering, ASCE* **139(11)**: 1951–1962.